

Adaptation of RainGaugeQC algorithms for quality control of rain gauge data from professional and non-professional measurement networks

Katarzyna Ośródk, Jan Szturc, Anna Jurczyk, Agnieszka Kurcz

Institute of Meteorology and Water Management – National Research Institute, ul. Podleśna 61, 01-673 Warsaw, Poland

Correspondence to: Jan Szturc (jan.szturc@imgw.pl)

Abstract. Rain gauge measurements are one of the primary techniques used to estimate a precipitation field, but they require careful quality control. This paper describes a modified RainGaugeQC system, which is applied to real-time quality control of rain gauge measurements made every 10 min. This system works operationally at the national meteorological and hydrological service in Poland. The RainGaugeQC algorithms, which have been significantly modified, are described in detail. The modifications were made primarily to control data from non-professional measurement networks, which may be of lower quality than professional data, especially in the case of personal stations. Accordingly, the modifications went in the direction of performing more sophisticated data control, applying weather radar data and taking into account various aspects of data quality, such as consistency analysis of data time series, bias detection, etc. The effectiveness of the modified system was verified based on independent measurement data from manual rain gauges, which are considered one of the most accurate measurement instruments, although they mostly provide daily totals. In addition, an analysis of two case studies is presented. This highlights various issues involved in using non-professional data to generate multi-source estimates of the precipitation field.

1 Introduction

1.1 Precipitation measurements

Precipitation is one of the most important meteorological parameters – due to its great practical importance in water management, flood control and other issues (e.g., Loritz et al., 2021; Sokol et al., 2021). For this reason, conducting measurements and estimating the precipitation field are very important tasks, though also very challenging because of the very high temporal and spatial variability of precipitation and its intermittent nature. The shorter the accumulation time of measurements, the greater the spatial variability of an estimated precipitation field and the greater its uncertainty (Berndt and Haberlandt, 2018; Bárdossy et al., 2021). This is especially true when estimating sub-daily totals and, even more the case for sub-hourly precipitation totals.

Until today, the basic measurements of precipitation are in situ measurements carried out by means of rain gauge networks, and this does not change despite the intensive development of remote sensing techniques, such as radar and satellite, from which measurements are distorted. From a hydrological perspective, rain gauge measurements are considered the most accurate, although they are limited to specific, rather sparsely distributed points. Consequently, when estimating the precipitation field, measurement data provided by different techniques are treated as independent estimates of the same physical quantity. Thus, the final estimate of a precipitation field,

37 which is often referred to as quantitative precipitation estimation (QPE), is determined using various methods of
38 combining data from different sources (multi-source estimation), taking into account the strengths and weaknesses
39 of each of these techniques (McKee et al., 2016; Jurczyk et al., 2020b).

40 Since all measurement techniques are subject to significant errors, which have a different temporal and spatial
41 structure, all rainfall measurements need advanced quality control (QC) (Szturc et al., 2022). This applies not only
42 to weather radar measurements (Lanza and Vuerich, 2009; Ośródko et al., 2014; Ośródko and Szturc, 2022; Sokol
43 et al., 2021), but also to rain gauge measurements. The latter are considered accurate at their locations, however
44 field experiments (Wood et al., 2000) and experiences with dual-sensor rain gauges (Ośródko et al., 2022) show
45 that trust in rain gauges is often excessive – errors in their measurements can sometimes be very significant.

46 Quality control of rain gauge data is carried out using various approaches, most commonly by analysing the
47 spatial and temporal distribution of measurements. As such information is insufficient for effective QC, especially
48 in the case of sparse measurement networks, external data from other measurement techniques, most often weather
49 radar and satellite, are used (Ośródko et al., 2022; Yan et al., 2024). Increasingly, deep learning techniques are
50 also being applied for QC (Sha et al., 2021). It should be noted that QC applied to short rainfall totals, such as the
51 10-min employed in this work, is considerably more difficult than for longer totals, such as 1-h (Villalobos-Herrera
52 et al., 2022).

53 Due to the particular importance of rain gauge measurements, especially for the adjustment (calibration) of
54 radar and satellite measurements, it is crucial when estimating the precipitation field that rain gauge networks are
55 as dense as possible (Hohmann et al., 2021). This implies a very high financial as well as technical and
56 organisational effort, so that a great deal of work is currently being done to deliver rain gauge data from other
57 networks, not only from the national meteorological and hydrological services (NMHSs). A separate issue is the
58 employment of “opportunistic” measurement techniques, i.e. precipitation data acquired from devices not
59 dedicated to rainfall measurement, e.g. by analysing the attenuation of signals in commercial microwave links
60 used in mobile phone networks, see e.g.: Chwala and Kunstmann (2019), Polz et al. (2020), Graf et al. (2021),
61 Pasierb et al., (2024).

62 **1.2 Non-professional rain gauge networks**

63 Apart from the rain gauge networks of the NMHSs, measurement networks set up and maintained by various
64 institutions – usually state or local authorities taking measurements for their own purposes – can also be a source
65 of rain gauge data. Another possibility is collecting meteorological measurements carried out by individual people
66 with generally low-cost measuring stations, for whom taking measurements, analysing them and comparing with
67 data generated by meteorological services is a hobby activity (Muller et al., 2015; Krennert et al., 2018; Zheng et
68 al., 2018). These are so-called personal or citizen weather stations (PWS or CWS).

69 For the purposes of this paper, all measurements carried out by institutions other than NMHSs are considered
70 “non-professional” because they do not guarantee compliance with the standards set by the World Meteorological
71 Organisation (WMO) (WMO-No. 488, 2010) to the same extent as NMHSs measurements. A distinction between
72 professional and non-professional rain gauges has been proposed by, among others, Garcia-Marti et al. (2023). In
73 addition, the aforementioned personal stations set up by individual hobbyists need to be distinguished, as direct
74 control of the location, technical conditions or maintenance of such stations is impossible in practice. Such stations
75 should be treated with less trust, and the uncertainty of the data is due to a number of reasons, which have been

76 described in detail in the literature (e.g. Bell et al., 2015; Båserud et al., 2020; Hahn et al., 2022; Urban et al.,
77 2024). Nevertheless, many studies show that such data can be a valuable source of precipitation information (de
78 Vos et al., 2017; 2019; Horita et al., 2018; Nipen et al., 2020; Bárdossy et al., 2021), thanks to the relatively large
79 number of these stations especially in urban areas, bearing in mind that professional gauges are typically located
80 outside city centres (Overeem et al., 2024).

81 The incorporation of non-professional data is associated with some overall increase in uncertainty in
82 precipitation data. Consequently, QC algorithms for these data should include not only the filtering out of clearly
83 erroneous measurements and a decrease of their quality metric in the form of e.g. a quality index (*QI*), but for less
84 supervised networks it is also necessary to correct at least the systematic errors associated with the bias of these
85 measurements.

86 **1.3 Overview of approaches to QC of rain gauge data**

87 The specificity of data from non-professional rain gauges is primarily due to the greater uncertainty of their
88 measurements. This entails the development of more sophisticated, but also more restrictive quality control
89 algorithms. These are generally extensions of the QC methods applied to data from NMHSs, but here they analyse
90 the reliability of individual measurements in more depth. These methods most often rely on verification with
91 professional rain gauges, but also use other measurement data, especially weather radar data.

92 *Spatial distribution of precipitation measurements* – detection of inconsistencies with surroundings. The most
93 common quality control techniques involve checking whether the deviation from the reference measurements,
94 which can also be data from nearby rain gauges, are within preset threshold values. If a measurement exceeds the
95 threshold, then it is treated as an outlier and either its quality index *QI* (or quality flag) is decreased or the
96 measurement is rejected (de Vos et al., 2017; Båserud et al., 2020). In addition, precipitation data from other
97 sources, primarily weather radar, can be used to quantify the uncertainty of outlying measurement data (Ośródk
98 and Szturc, 2022). Spatial consistency tests are very difficult to perform for a sparse rain gauge network, so the
99 QC in terms of spatial consistency may not be carried out, and in the case of personal rain gauges, such data may
100 simply be rejected (Nipen et al., 2020). Alerskans et al. (2022) used a cost function based on a contingency table,
101 which optimises the parameters of the spatial QC algorithm used to detect as many actually erroneous data as
102 possible, while minimising the number of correct data that were found to be erroneous.

103 *Correlation of time series of precipitation measurements with reference data.* The temporal consistency check
104 involves detecting stations from which measurements often have relatively low reliability, but not so much that
105 individual measurements do not pass a spatial consistency check. Analysis of the temporal consistency of rainfall
106 data is most often carried out by analysing the correlation of the time series from the controlled rain gauge with
107 the time series of reference data (Bárdossy et al., 2021; de Vos et al., 2019). Reference data can be either data from
108 professional rain gauges of relatively high quality or from other measurement techniques, primarily weather radar
109 (de Vos et al., 2019), but only after quality control (WMO-No. 1257, 2024). However, the use of radar data is
110 associated with difficulties, most often due to errors in estimation of the precipitation field (Ośródk
111 and Szturc, 2022). Moreover, weather radar measurements are performed at certain heights above the
112 ground surface – from a few hundred metres to as much as a few kilometres – and are then spatially averaged.
113 Analysis of the correlation coefficient of a time series becomes difficult, especially in cases where the rain gauge
114 reports false zero values (no precipitation) due to e.g. a sensor being blocked or some object obstructing the path

115 of the rain (e.g. buildings, vegetation). Another difficulty is caused by non-rainfall periods – time series with
116 predominantly very low rainfall can sometimes disturb the correlation, so a minimum precipitation threshold
117 should be used to filter out data from such periods (Hahn et al., 2022).

118 *Detection and removal of bias in precipitation measurements.* The approaches to the issue of quality control
119 of rain gauge data described above do not correct erroneously measured values, but only reduce their *QI* or remove
120 them. However, data correction is an important part of data quality control. First of all, it is about bias correction
121 (unbiasing), which most often results from rainfall underestimation related to rain gauge technology: rain gauge
122 measurements are underestimating the true rainfall due to wind-induced errors, wetting losses, evaporation losses,
123 trace precipitation, etc. The magnitude of the underestimation also depends on the construction of the rain gauge;
124 in particular, tipping-bucket devices are subject to significant bias (Segovia-Cardozo et al., 2021). This bias can
125 be eliminated, or at least reduced, by, for example, quantitatively analysing all underestimation factors and
126 introducing all important corrections (Zhang et al., 2019). Such adjustments, however, are generally conservative
127 because of the difficulty of considering all relevant factors and the lack of precise data on influencing parameters.
128 Another way is to compare non-professional measurements with a benchmark as reliable as possible, which could
129 be manual rain gauges, preferably lysimetric ones that measure at ground level (Haselow et al., 2019; Schnepper
130 et al., 2023). However, such measurements are not common, so remote sensing data such as radar observations,
131 which are more widely available, can be used as a benchmark, but they require the QC to have been previously
132 carried out. Unbiasing is also calculated on the basis of a larger data set collected during precipitation events
133 typical of the local climate (e.g. from 14 days, see de Vos et al., 2019). The bias factor determined on this basis is
134 treated as a climatological quantity.

135 **1.4 Structure of the paper**

136 This paper presents the RainGaugeQC system (Ośródką et al., 2022) after its adaptation for quality control of rain
137 gauge data from non-professional stations. The paper is structured as follows: after Section 1, Section 2 briefly
138 describes the different kinds of precipitation data on which the RainGaugeQC was developed and verified. Section
139 3 presents the algorithms of the RainGaugeQC system with the emphasis on solutions that are more advanced
140 when compared to the earlier version of the system. Results obtained over several months, as well as analysis of
141 two case studies, are discussed in Section 4. Section 5 summarises the paper with a list of conclusions resulting
142 from the use of the modified RainGaugeQC system.

143 **2 Precipitation data**

144 **2.1 Available networks of rain gauges**

145 IMGW operationally utilises telemetric rain gauge data from the following measurement networks operated by
146 (Fig. 1):

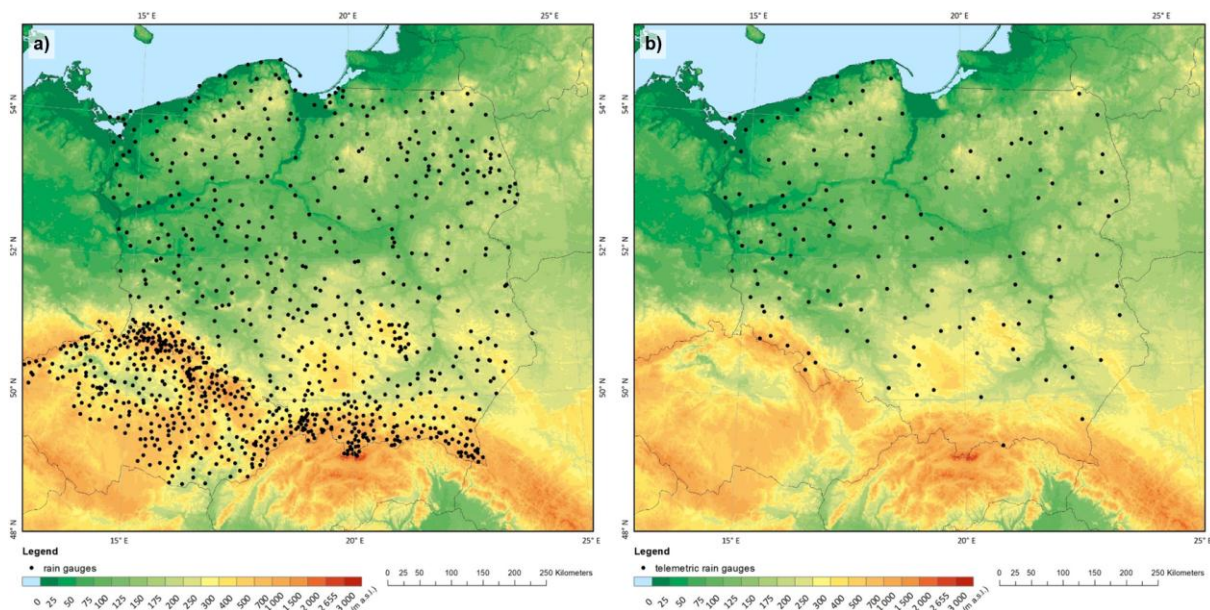
- 147 • IMGW (Institute of Meteorology and Water Management – National Research Institute) – network of
148 NMHS in Poland (<https://hydro.imgw.pl/#/map>).
- 149 • CHMU (Czech Hydrometeorological Institute) – network of NMHS in the Czech Republic. IMGW uses
150 data from stations near the Polish border
151 (https://www.chmi.cz/files/portal/docs/meteo/ok/images/srazkomerne_stanice_en.gif).

152 • General Directorate of the State Forests (DLP) – network of the meteorological monitoring program of
 153 forest areas (<https://www.traxelektronik.pl/pogoda/las/>).

154 The above data are used to generate operationally (in real-time) a multi-source precipitation field with high
 155 spatial resolution, which is the basis for generating nowcasting precipitation forecasts.

156 Synthetic information about the above networks is summarised in Table 1.

157



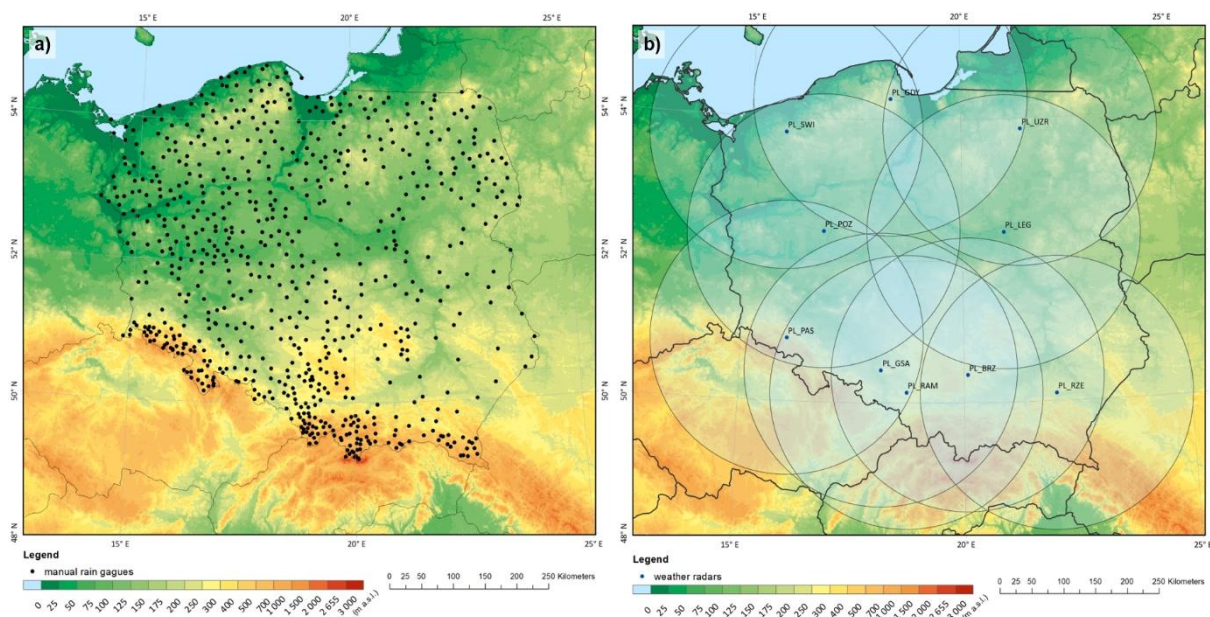
158
 159 **Figure 1: Telemetric rain gauge networks: a) IMGW and CHMU, b) State Forests.**

160
 161 **Table 1. Rain gauge networks incorporated into operational processing by RainGaugeQC system and**
 162 **estimation of precipitation field (as of October 2024).**

| ID | Network operator | Number of stations | Type of rain gauges | Type of network |
|----|--|--|---|------------------|
| 1 | IMGW | 656 | Heated and unheated, mostly two tipping bucket sensors, others weighing | Professional |
| 2 | CHMU | 324 stations located close to Polish territory | Heated, mostly tipping bucket sensors | Professional |
| 3 | General Directorate of the State Forests (DLP) | 145 | Heated, tipping bucket sensors | Non-professional |

163
 164 For the domain of Poland data from professional rain gauge networks operated by NMHSs in Poland (IMGW)
 165 and the Czech Republic (CHMU) are available. As the territory of the Czech Republic covers a large part of the
 166 analysed domain and, above all, a significant number of rain gauges are located close to mountainous areas on the
 167 border with Poland (Fig. 1), these data are very important for improving the reliability of the estimation of the
 168 precipitation field in southern Poland. The third network, belonging to the State Forestry Authority, is a non-
 169 professional research network so it is uncertain whether all the standards of the WMO recommendations are
 170 followed (WMO-No. 488, 2010).

171 The quality of precipitation data is highly dependent on the type of measuring devices being used. Currently,
 172 the IMGW network is still dominated by tipping-bucket type rain gauges, which are considered significantly less
 173 accurate than weighing rain gauges (e.g., Colli et al., 2014; Hoffmann et al., 2016).
 174



175
 176 **Figure 2: Computational domain of Poland with: a) IMGW's network of manual rain gauges, b) plotted 215-km ranges**
 177 **of weather radars of the Polish POLRAD radar network (as of July 2024).**

178
 179 A network of Hellmann-type manual rain gauges, providing independent reference data, is used in this study
 180 to verify the performance of the developed QC algorithms. As the data from these rain gauges are not available in
 181 real time, they cannot be used for rainfall field estimation or operational QC of telemetric data. The IMGW network
 182 consists of about 641 manual rain gauges, which provide daily rainfall accumulations (Fig. 2a). These data are
 183 believed to be much more accurate than measurements from telemetric rain gauges, which has been confirmed by
 184 extensive reliability analyses of different types of rain gauges at IMGW (Urban and Strug, 2021). They are
 185 subjected to manual QC before being used.

186 2.2 Weather radar precipitation data

187 Precipitation data from weather radars play a major role in the RainGaugeQC system for quality control of rain
 188 gauge data (Ośródk et al., 2022). The data used in this study are provided by the Polish POLRAD radar network
 189 operated by IMGW. The network consists of ten Doppler polarimetric radars working in C-band, manufactured by
 190 Leonardo Germany (Fig. 2b). Three-dimensional raw data and two-dimensional products are generated by the
 191 Rainbow 5 system every 5 min with 1-km spatial resolution and a range of 250 km. For the estimation of the
 192 precipitation field, data up to 215 km from the radar are used. This distance represents a balance between achieving
 193 the shortest possible range and ensuring complete coverage of the entire country with measurements.

194 The raw 3D radar data are quality controlled and corrected by the RADVOL-QC system (Ośródk et al., 2014;
 195 Ośródk and Szturc, 2022). The product used to estimate the rainfall field is PseudoSRI (Pseudo Surface Rainfall
 196 Intensity): cut-off at 1-km altitude above ground and from the lowest elevation out of the SRI range, generated

197 every 5 min and accumulated into 10-min sums taking into account spatio-temporal interpolation between two
198 adjacent measurements. As a result of quality control with the RADVOL-QC system, the corresponding *QI* quality
199 index fields are also assigned to the individual estimated precipitation fields. In addition, some kind of quality
200 control of radar precipitation takes place at the stage when data from individual radars is combined into composite
201 maps. This is done by means of an algorithm that takes into account the time-varying spatial distribution of the
202 quality index (Jurczyk et al., 2020a).

203 Due to the bias present in the weather radar observations, these data are adjusted with rain gauge data, but only
204 from the professional networks, derived from the 1-h moving window. However, if a precipitation accumulation
205 is below a preset threshold, then this period is extended accordingly, up to a maximum of the seasonal
206 accumulation. This adjustment is carried out from gauge-radar ratios determined at rain gauge locations, spatially
207 interpolated over the entire domain.

208 **2.3 Multi-source precipitation estimates RainGRS**

209 Multi-source precipitation field estimates are generated by the RainGRS system of IMGW. The system combines
210 rain gauge, weather radar, and satellite precipitation data in real time (Szturc et al., 2018; Jurczyk et al., 2020b;
211 2023). The algorithm for combining these data is based on conditional merging according to an algorithm proposed
212 by Sinclair and Pegram (2005), which attempts to enhance the strengths and reduce weaknesses of individual
213 measurement techniques. This approach was modified in RainGRS by taking into account the quantitative
214 information about the spatial distribution of the quality of the individual input data (quantified by *QI*). These
215 estimates are produced every 10 min with a high spatial resolution of 1 km x 1 km.

216 In the study, two versions of multi-source RainGRS precipitation estimates are generated in order to examine
217 the impact of incorporating non-professional data. In the first version, rain gauge data only from the professional
218 networks of IMGW and CHMU were taken, while in the second version, data from the non-professional network
219 of the State Forests were added to this set.

220 **3 RainGaugeQC system for QC of rain gauge data**

221 **3.1 RainGaugeQC system for QC of rain gauge data from a professional network**

222 The RainGaugeQC system was originally designed to perform real-time quality control of rain gauge data from
223 measurement networks maintained by IMGW. This system was described in detail in work by Ośródko et al.
224 (2022), so in this study, after a very concise presentation of the algorithms, the following sections will describe
225 only modifications made to adapt it to data from non-professional networks.

226 In the standard version of RainGaugeQC (Ośródko et al., 2022) (see column “Before modification” in Table
227 2), firstly the simple plausibility tests – the gross error check (GEC) and range check (RC) – were performed on
228 individual measurements. The GEC involves detecting when natural limits are exceeded, while the RC focuses on
229 identifying when climate-based thresholds are surpassed at an individual gauge. Then the more complex checks
230 were conducted using a larger amount of rain gauge data from either a specific time range or a specific area, as
231 well as using external data provided by weather radars. Firstly, the Radar Conformity Check (RCC) was applied
232 to identify false precipitation on the basis of the radar measurements. Obstruction or blocking of the sensors was
233 also checked for. Next, the Temporal Consistency Check (TCC) was performed, but this version was designed

234 only for dual-sensor stations: data from the pairs of rain gauge sensors were tested for the existence of significant
 235 differences between them. The most advanced algorithm was the Spatial Consistency Check (SCC) which
 236 identified outliers by comparing observed values with data from neighbouring stations.

237 An important outcome of the system was the determination of the quality index (*QI*) of analysed data, which
 238 is a unitless value with a range [0.0, 1.0], where “0.0” means extremally bad data and “1.0” means perfect data. At
 239 each time-step this *QI* metric was determined by the RainGaugeQC for each sensor and then the sensor with the
 240 highest quality is taken for further processing.

241

242 **Table 2. A summary of the quality control algorithms used in the RainGaugeQC system before and after**
 243 **modification.**

| Abbr. | Algorithm | Before modification | After modification |
|-------|----------------------------|---|---|
| GEC | Gross Error Check | Gross errors | |
| RC | Range Check | Exceeding climatological thresholds | |
| RCC | Radar Conformity Check | Detection of false rainy and non-rainy events | |
| BSC | Blocked Sensor Check | Detection of blocked sensors | |
| TCC | Temporal Consistency Check | Comparison of two sensors | Time series comparison with weather radar data |
| BC | Bias Check | – | Detection and correction of bias with adjusted radar data |
| SCC | Spatial Consistency Check | Detection of outliers from the local vicinity | Detection of outliers from the local vicinity (updated) |

244

245 3.2 Directions of development in RainGaugeQC

246 The possibility of incorporating non-professional data at IMGW became a motivation for more sophisticated data
 247 quality control. The QC algorithms in the previous version of RainGaugeQC turned out to be inadequate for non-
 248 professional data, as these gauges are generally not dual-sensor. On the other hand, the inclusion of new data
 249 significantly improved the performance of the SCC algorithm due to the higher density of the measurement
 250 network. Therefore, it was necessary to redesign the RainGaugeQC system in order to adapt it to rain gauge
 251 networks equipped with different types of sensors, supervised to various degrees, so that the system became more
 252 universal. The modified algorithms tailored to the new challenges associated with incorporating non-professional
 253 data are summarised in Table 2 in the “After modification” column. Here is a brief overview of the changes made
 254 to the RainGaugeQC algorithms, whereas detailed information can be found in Sections 3.3 to 3.5.

255 *TCC*. In the new version of the TCC (time series comparison with adjusted weather radar data) algorithm,
 256 weather radar data is used to compare time series from a specific time interval to check the correlation between
 257 rain gauge measurements and radar observations. The correlation coefficient is used as a metric for the relevant
 258 component of the quality index of the rain gauge data. This allows for a reduction in the data quality index of rain
 259 gauges with measurements disturbed for a certain time period due to failure, poor maintenance or bad location.

260 *BC*. The above TCC algorithm is not sensitive to the bias of rain gauge measurements, so the BC (bias check
 261 with adjusted radar data) algorithm is used to detect bias in the data. It also works by analysing long-term data

262 series, but in this case they are used to compare data accumulations from rain gauges with radar accumulations.
263 The quantitative estimation of the bias of the rain gauge data allows relevant components of the quality index to
264 be determined. In the case of personal rain gauges, unbiasing is carried out as well as reducing the QI value.

265 *SCC*. The *SCC* (detection of outliers from the local vicinity) algorithm was already introduced in the first
266 version of the RainGaugeQC system, but significant modifications have been made to the current version. It detects
267 outliers, i.e. the measurements at a given time-step which deviate from the values from rain gauges located in a
268 certain area. The increase in the number of rain gauges through incorporating non-professional data has made it
269 easier to determine the degree to which individual data is an outlier. The quality index reduction for outliers is
270 quantified on the basis of the spatial variability of the precipitation field derived from the radar data.

271 All parameters of the algorithms described in sections 3.3 to 3.5 were chosen empirically by comparing the
272 calculated QI values with the expected ones based on our assessment of the data reliability.

273 **3.3 New version of TCC algorithm (Time series comparison with weather radar data)**

274 The TCC algorithm is designed to eliminate erroneous rain gauge measurements (G) by analysing the correlation
275 on time series. The reference is radar precipitation (R) after adjustment with rain gauge observations only from
276 professional networks.

277 For the calculation, pairs of rain gauge (G) and radar (R) data are taken if at least one of the values is greater
278 than 0.025 mm, and their quality index (QI) is at least 0.7 for G and 0.8 for R . Two time series aggregated from
279 10-min accumulations: “short” and “long” comprising 5 and 10 days, respectively, are analysed in order to test
280 correlations on time series that are as short as possible and, on the other hand, sufficiently representative. The
281 number of non-precipitation pairs c_{dry} for long series is determined provided that both values are less than 0.025
282 mm. For each series, hourly accumulations are determined and then the number of measurement pairs c and
283 correlation coefficient r are calculated.

284 The procedure for assessing data quality is carried out by checking a list of conditions. For a given measurement
285 these conditions are examined sequentially and, depending on the result, further ones are checked or the quality
286 index is reduced accordingly.

287 First, the 10-day radar precipitation total $\sum_{10\ days}(R)$ is checked. If this is too low, then the correlation
288 coefficient is not calculated, as it may not be reliable in such a case. In addition, it is checked whether the rain
289 gauge rainfall $\sum_{10\ days}(G)$ differs significantly from the radar data (formulae 1 and 2) and depending on this, the
290 quality index of G is reduced.

291 If the both accumulations are below the assumed threshold values, then the quality index of the rain gauge data
292 is not reduced and the check is stopped:

$$293 \quad (\sum_{10\ days}(R) < 3.0) \text{ and } (\sum_{10\ days}(G) < 6.0) \rightarrow \text{TCC stopped} \quad (1)$$

294 If the amount of radar precipitation for the long series is below the assumed threshold and the amount of rain
295 gauge precipitation is above the corresponding threshold, indicating large differences between the two
296 accumulations, then the check is also stopped and the quality index of the rain gauge data is reduced by 0.05:

$$297 \quad (\sum_{10\ days}(R) < 3.0) \text{ and } (\sum_{10\ days}(G) \geq 6.0) \rightarrow \text{TCC stopped, } QI = QI - 0.05 \quad (2)$$

298

299 The check is passed if the number of measurement pairs is above the preset threshold and correlation coefficient
 300 r is above 0.3 for short or long series. Then the quality index is reduced on the basis of the relevant correlation
 301 coefficient, according to the following formula:

$$302 \quad (c > 6) \text{ and } (r > 0.3) \rightarrow \text{TCC passed, } QI = \begin{cases} QI & r > 0.85 \\ QI - \frac{1-r}{4} & r \leq 0.85 \end{cases} \quad (3)$$

303 If there is an insufficient number of measurements for short series and at the same time the number of non-
 304 precipitation data pairs is above a preset threshold, indicating that there is a longer non-precipitation period, then
 305 the TCC is stopped and quality index is reduced:

$$306 \quad (c_{dry} > 1000) \text{ and } (c_{short} \leq 6) \rightarrow \text{TCC stopped, } QI = QI - 0.05 \quad (4)$$

307 Finally, the number of measurements and correlation coefficient with radar data for short and long periods are
 308 examined. If the condition in Formula 5 is met then the check is stopped. If not, the check is failed:

$$309 \quad [(c \leq 6) \text{ or } (r = \text{"no data"})] \rightarrow \text{TCC stopped, } QI = QI - 0.05 \quad (5)$$

$$310 \quad \text{else} \rightarrow \text{TCC failed, } QI = QI - 0.3.$$

311 This formula applies to cases when there are too few measurements, or the correlation coefficient could not be
 312 calculated or was below the assumed threshold for short or long series.

313 **3.4 New algorithm BC (Detection of bias with adjusted radar data)**

314 The determination of bias in the BC algorithm is carried out by comparing the precipitation accumulations obtained
 315 from the time series recorded on a given rain gauge with adjusted radar rainfall as a reference. For the most recent
 316 10 days using a 10-min temporal resolution, rain gauge and radar precipitation accumulations, denoted as ΣG and
 317 ΣR respectively, are calculated from gauge-radar pairs, for which both measurements have a quality index of at
 318 least 0.7 for G and 0.8 for R .

319 Choice of the length of the precipitation accumulation period to determine the bias is not a trivial issue. Long
 320 accumulations better reflect the overall uncertainty of the measurements at a given station, but, on the other hand,
 321 short accumulations better follow the current precipitation characteristics during a particular precipitation event.
 322 Most often, bias is determined on rainfall accumulations from up to a few dozen hours, but sometimes on much
 323 longer accumulations – e.g. Yousefi et al. (2023) used seasonal totals to unbiased radar data with rain gauge data.
 324 The *bias* of the rain gauge measurements is calculated from the ratio of radar to rain gauge precipitation
 325 accumulations:

$$326 \quad \text{bias} = \frac{\Sigma R}{\Sigma G} \quad (6)$$

327 The bias determined in this way is used to reduce the quality index QI of the controlled rain gauge data. If the
 328 precipitation accumulations ΣG and ΣR are similar, which is checked using the corresponding similarity function,
 329 the quality of the measurement remains unchanged. The similarity function is defined as follows:

$$330 \quad SF(\Sigma G, \Sigma R) = \begin{cases} \text{true} & 1.3 \cdot \min(\Sigma G, \Sigma R) + 7.0 > \max(\Sigma G, \Sigma R) \\ \text{false} & 1.3 \cdot \min(\Sigma G, \Sigma R) + 7.0 \leq \max(\Sigma G, \Sigma R) \end{cases} \quad (7)$$

331 If the radar and rain gauge precipitation accumulations for a given rain gauge are not similar, then depending
 332 on the bias determined from Formula 6, the value of the quality index QI of a given measurement is reduced, but
 333 to a varying extent, according to the formula:

$$334 \quad QI = \begin{cases} QI - 0.05 & bias \in \left[\frac{1}{5}, 5\right] \\ QI - 0.2 & bias \in \left[\frac{1}{10}, \frac{1}{5}\right) \text{ or } bias \in (5, 10] \\ QI - 0.5 & bias \in \left[\frac{1}{20}, \frac{1}{10}\right) \text{ or } bias \in (10, 20] \\ QI - 1.0 & bias \in \left(0, \frac{1}{20}\right) \text{ or } bias \in (20, +\infty) \end{cases} \quad (8)$$

335 In case when the bias cannot be estimated, the quality index of a particular measurement is reduced according
 336 to the formula:

$$337 \quad QI = \begin{cases} QI - \min\left(1.0, \frac{|\Sigma G - \Sigma R|}{10.0}\right) & (\Sigma G = 0.0) \text{ or } (\Sigma R = 0.0) \\ QI - 0.2 & (\Sigma G = \text{"no data"}) \text{ and } (\Sigma R = \text{"no data"}) \end{cases} \quad (9)$$

338 In terms of data from personal weather stations, they are considered to be subject to much greater uncertainty
 339 due to the lack of supervision of the technical condition of the rain gauges, poor maintenance, bad location, etc.
 340 Such stations should therefore be treated more rigorously than stations supervised by the institutions responsible
 341 for the measurements. The similarity function (Formula 7) is not applied, as their quality index values are always
 342 reduced by the formula:

$$343 \quad QI = \begin{cases} QI - 0.1 & bias \in \left[\frac{1}{5}, 5\right] \\ QI - 0.3 & bias \in \left[\frac{1}{10}, \frac{1}{5}\right) \text{ or } bias \in (5, 10] \\ QI - 0.7 & bias \in \left[\frac{1}{20}, \frac{1}{10}\right) \text{ or } bias \in (10, 20] \\ QI - 1.0 & bias \in \left(0, \frac{1}{20}\right) \text{ or } bias \in (20, +\infty) \end{cases} \quad (10)$$

344 when $bias$ cannot be estimated, the quality index value of a given measurement is reduced by the formula:

$$345 \quad QI = \begin{cases} QI - \min\left(1.0, \frac{|\Sigma G - \Sigma R|}{10.0}\right) & (\Sigma G = 0.0) \text{ or } (\Sigma R = 0.0) \\ QI - 0.4 & (\Sigma G = \text{"no data"}) \text{ and } (\Sigma R = \text{"no data"}) \end{cases} \quad (11)$$

346 In addition, unbiasing should be performed for data from personal stations, which is not done for other types
 347 of stations, as they only have a reduced QI . Unbiasing is performed on the basis of the bias determined from
 348 Formula 6, but limiting its value to factor 4:

$$349 \quad bias_4 = \begin{cases} \frac{1}{4} & bias \leq \frac{1}{4} \\ bias & \frac{1}{4} < bias \leq 4 \\ 4 & bias > 4 \end{cases} \quad (12)$$

350 The above limitation on the value of the $bias_4$ factor is to protect against too large a change in the value of the
 351 corrected precipitation (van Andel, 2021).

352 Finally, the unbiased precipitation accumulation G_{cor} is determined from the formula:

$$353 \quad G_{cor} = bias_4 \cdot G \quad (13)$$

354 As IMGW does not yet have a sufficiently dense network of cooperating personal stations (Drożdżoń and
 355 Absalon, 2023), tests have not been carried out to verify the algorithm designed in this study on data from such a
 356 network.

357 3.5 Updated SCC algorithm (Detection of outliers from the local vicinity)

358 The spatial methods for quality control, such as the SCC, are especially effective for dense rain gauge networks
 359 because they utilise observations from nearby stations (Alerskans et al., 2022). Thus, when applied to sparse
 360 networks, it is more likely that a correct value measured by a rain gauge will be classified as erroneous in the case
 361 of intense convective rainfall of a very local nature.

362 Based on the analysis of the performance of the SCC algorithm – as published in a previous paper on the
 363 standard version of RainGaugeQC system (Ośródką et al., 2022) in Appendix C – a modification was made in
 364 relation to the degree of QI reduction depending on the spatial variability of rainfall.

365 The algorithm has not changed in terms of assigning each rain gauge measurement to one of the three classes
 366 of outliers: strong, medium, and weak, or to the class of correct data. However, the algorithm for reducing the QI
 367 value of each measurement assigned to any of the outlier classes was modified. In the current version of the
 368 algorithm, the magnitude of QI reduction depends on whether a given rain gauge measurement is within an area
 369 of a high spatial variability of precipitation determined from weather radar data of sufficient quality $QI(R)$. In this
 370 case, the outlier is treated less restrictively. The concept of spatial variability function (SVF) was introduced for
 371 this purpose, and is defined as follows:

$$372 \quad SVF = \frac{SVF_{mean}(R_{mean}) + SVF_{var}(R_{var})}{2} \quad (14)$$

373 The SVF consists of two components indicating the degree of spatial variability of the precipitation:

$$374 \quad SVF_{mean}(R_{mean}) = \begin{cases} 1 & R_{mean} \geq 1.0 \text{ mm} \\ \frac{R_{mean} - 0.1 \text{ mm}}{1.0 \text{ mm} - 0.1 \text{ mm}} & 0.1 \text{ mm} < R_{mean} < 1.0 \text{ mm} \\ 0 & R_{mean} \leq 0.1 \text{ mm} \end{cases} \quad (15)$$

$$375 \quad SVF_{var}(R_{var}) = \begin{cases} 1 & R_{var} \geq 1.0 \text{ mm}^2 \\ \frac{R_{var} - 0.03 \text{ mm}^2}{1.0 \text{ mm}^2 - 0.03 \text{ mm}^2} & 0.03 \text{ mm}^2 < R_{var} < 1.0 \text{ mm}^2, \\ 0 & R_{var} \leq 0.03 \text{ mm}^2 \end{cases}$$

376 where R_{mean} is the mean radar precipitation (in mm) for wet pixels in the 100 km x 100 km subdomain including
 377 25 km margins (see: Ośródką et al., 2022); R_{var} is the mean variance of radar precipitation (in mm^2) in the
 378 subdomain calculated analogously to R_{mean} .

379 On the basis of the value of the SVF function, the reduction in the quality index for individual rain gauge
 380 observation is determined, according to its classification into a specific outlier class (see: Ośródką et al., 2022):

$$381 \quad QI = \begin{cases} QI - (0.30 \cdot (1 - SVF) + 0.10 \cdot SVF) & \text{strong outlier} \\ QI - (0.20 \cdot (1 - SVF) + 0.05 \cdot SVF) & \text{medium outlier} \\ QI - 0.10 \cdot (1 - SVF) & \text{weak outlier} \end{cases} \quad (16)$$

382 3.6 Determination of *QI*

383 Before all the checks, each rain gauge observation is assigned the perfect *QI* value (1.0). Depending on the result
384 of a particular QC algorithm, the *QI* of an examined measurement is decreased by a relevant value. If the final *QI*
385 value, i.e. after all checks, is below a preset threshold, the observation is considered useless and is replaced with
386 “no data”.

387 4 Analysis of the RainGaugeQC system performance on non-professional data

388 The performance of the RainGaugeQC system, designed to control the quality of precipitation data from
389 professional and non-professional rain gauge networks, is shown through a comparison of the statistics calculated
390 for these two rain gauge networks:

- 391 • professional network of IMGW, the Polish NMHS, supplemented in the border region by data from
392 CHMU, which is the Czech NHMS,
- 393 • non-professional network of the General Directorate of the State Forests.

394 The most important characteristics of these networks are summarised in Table 1, and the locations of the rain
395 gauges are shown in Fig. 1. Rain gauges from personal networks have not been included, as the establishment of
396 their network at IMGW is still at a preliminary stage.

397 The analysis was carried out for four months – April, July, October 2023 and January 2024 – considered typical
398 of the four seasons. The summer season (July) is dominated by convective precipitation, which is often intense
399 and highly variable in time and space, while the winter season (January) is dominated by stratiform precipitation,
400 often in the form of snow. In the intermediate seasons (April, October) precipitation is less intense – it is
401 generally rain, and is rarely convective.

402 4.1 Verification metrics

403 The reliability of the precipitation estimates generated using the RainGaugeQC system was verified by
404 comparison with the reference precipitation accumulations from manual rain gauges that are treated as the closest
405 to the true precipitation at their locations. The following metrics were employed:

- 406 • Pearson correlation coefficient:

$$407 \quad CC = \frac{\sum_{i=1}^n (E_i - \bar{E})(O_i - \bar{O})}{\sqrt{\sum_{i=1}^n (O_i - \bar{O})^2 \sum_{i=1}^n (E_i - \bar{E})^2}} \quad (17)$$

- 408 • root mean square error:

$$409 \quad RMSE = \sqrt{\frac{1}{n} \sum_{i=1}^n (E_i - O_i)^2} \quad (18)$$

- 410 • root relative square error:

$$411 \quad RRSE = \frac{\sqrt{\sum_{i=1}^n (E_i - O_i)^2}}{\sqrt{\sum_{i=1}^n (O_i - \bar{O})^2}} \quad (19)$$

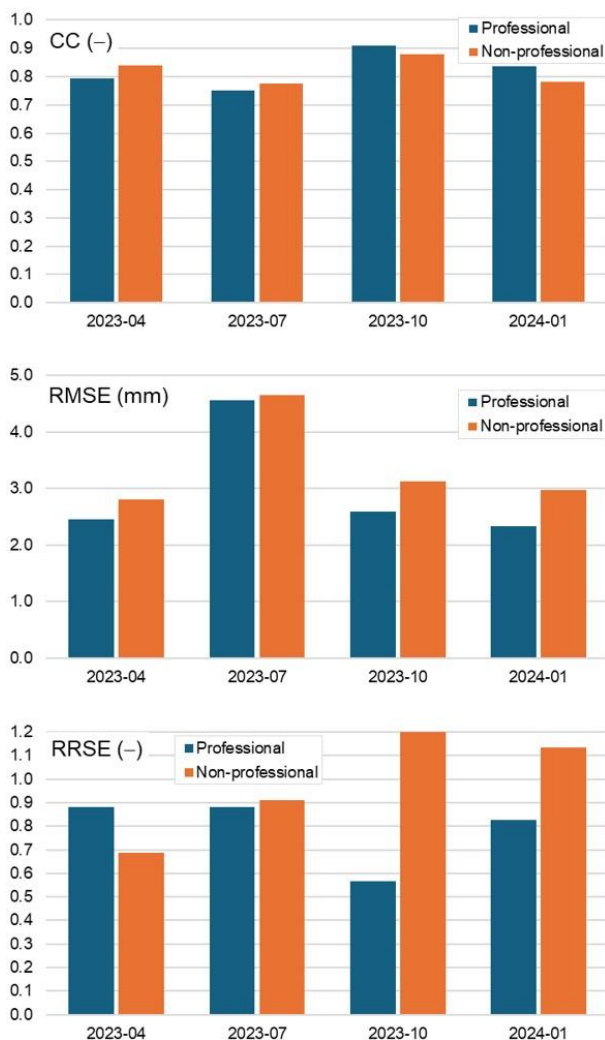
- 412 • statistical bias:

413
$$\text{BIAS} = \frac{1}{n} \sum_{i=1}^n (E_i - O_i) \tag{20}$$

414 where E_i is the estimated value, O_i is the reference value, i is the gauge number, n is the number of gauges, whereas
 415 \bar{E} and \bar{O} are the mean values of E_i and O_i , respectively.

416 **4.2 Non-professional versus professional rain gauge data**

417 A comparison of reliability metrics of precipitation estimates obtained from a network of professional and non-
 418 professional rain gauges, respectively, is shown in Fig. 3. Point measurements of rainfall were verified against
 419 values at rain gauge locations obtained from the interpolation of manual rain gauges using the inverse distance
 420 weighting method. Professional rain gauges situated at manual gauge locations, a relatively common situation in
 421 the IMGW network, were not included in the statistics in order not to favour this category of data. Therefore,
 422 around 200 professional rain gauges were used for verification instead of all 469. Days with precipitation
 423 accumulation below 0.5 mm were not included in the calculations (in total 21 days in these four months).
 424



425
 426 **Figure 3: Reliability statistics of rainfall estimates calculated for data obtained from the network of professional (navy)**
 427 **and non-professional (orange) rain gauges. Spatially interpolated manual rain gauges are used as a reference. Data**
 428 **from April, July, October 2023 and January 2024.**

429

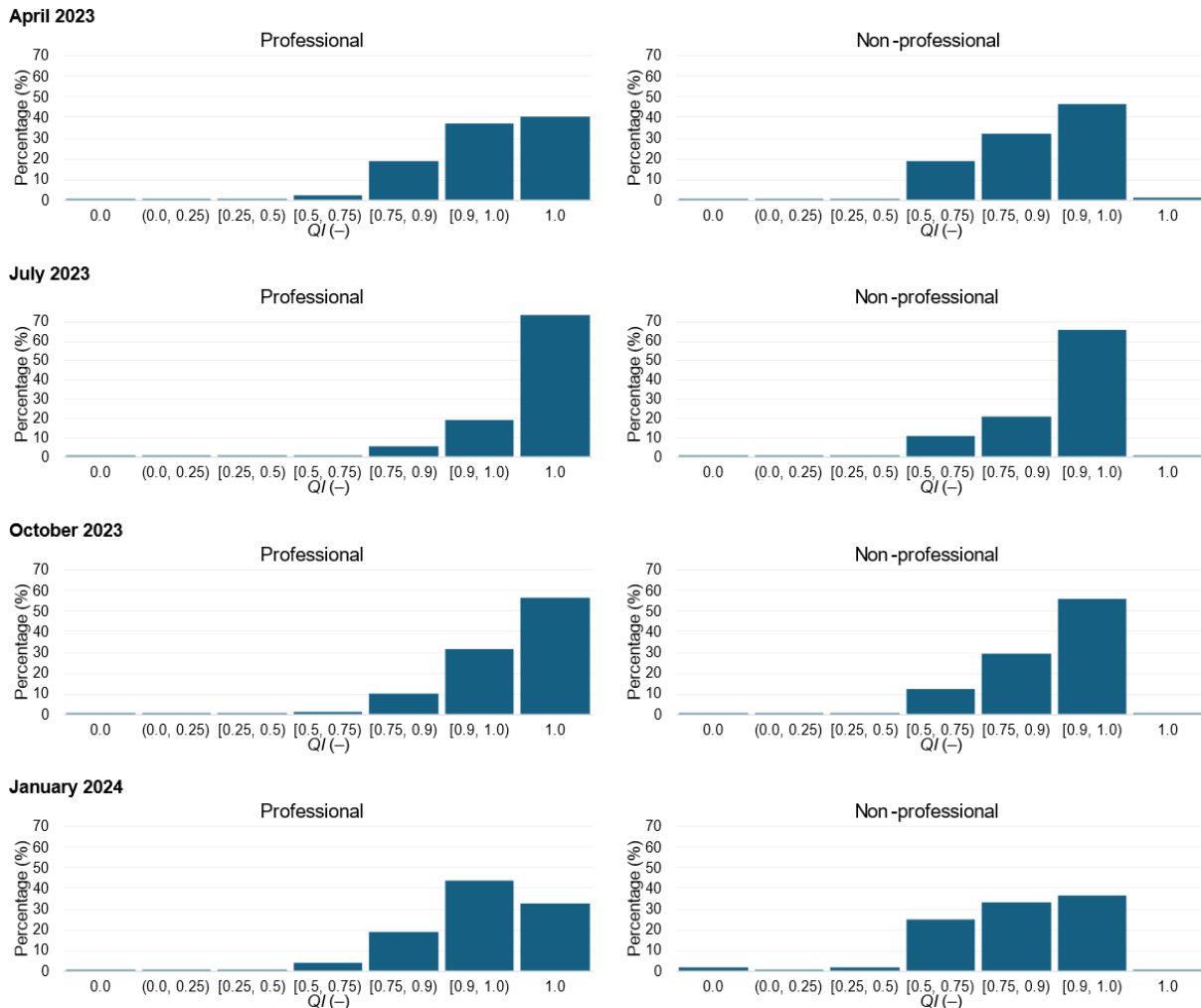
430 The reliability of the non-professional data in general is close to that of the professional data, especially as
431 regards the correlation coefficient: on average for both it is about 0.82, and the differences between them are small,
432 at below 0.06. The RMSE metric related to the deviation from the reference data is already clearly worse for the
433 non-professional data, by on average about 0.41 mm. The largest difference was found for January, when it reached
434 0.65 mm. Only in the summer period (July) is the difference between the non-professional and professional data
435 small (0.09 mm), though the error values are highest at that time (4.65 and 4.55 mm, respectively). During this
436 period, convective precipitation is frequent, more intense, and also more dynamic, and as a consequence, the
437 comparison with spatially interpolated reference data can produce large differences. In contrast, a similar but
438 relative RRSE metric gives less conclusive results: in April it is much better for the non-professional data (0.69
439 versus 0.88), while in the other months the non-professional data are worse than the professional, with a significant
440 difference of 0.63 in October.

441 **4.3 Comparison of the QC system performance on professional and non-professional data**

442 In this Section an examination is made of the extent to which the *QI* of rain gauge data for professional and non-
443 professional stations is reduced by the RainGaugeQC system in different months of the year. The *QI* plays a key
444 role in the multi-source precipitation field estimation performed by the RainGRS system as the *QI* index is one of
445 the most important weights during spatial interpolation of rain gauge data and, most importantly, it is a weight
446 when rain gauge data is combined with the other precipitation estimates – radar and satellite-based. As a result of
447 this approach, the impact of low-quality data on the final precipitation field estimate can be reduced.

448

449



450
 451 **Figure 4: Percentages of data with QI values in different ranges (histograms). Data from April, July, October 2023 and**
 452 **January 2024.**

453
 454 Fig. 4 summarises the percentage of rain gauge data in different ranges of QI values assigned to individual
 455 measurements as a result of QI performed with a modified version of the RainGaugeQC system for four months
 456 representing different seasons, separately for professional and non-professional stations. It can be noted that, in
 457 general, QI values are significantly higher for professional data, meaning that QC algorithms indicate higher
 458 uncertainty in non-professional data. While unreduced quality ($QI = 1.0$) characterises 32.5 – 57.6% of all
 459 professional data depending on the season, just 26.0 – 57.6% of non-professional data. On the other hand, lower
 460 quality values ($QI < 0.75$) at different seasons characterise 1.4 – 4.9% of the professional data and 7.4 – 24.2% of
 461 the non-professional data. Probably the reason for the worse results for January is the occurrence of snowfall,
 462 which is more challenging for radars to detect.

463 There is noticeable seasonal dependence of the number of data with QI in specific value ranges, which is similar
 464 for professional as well as non-professional data. The highest percentage of data with a QI of exactly 1.0, i.e.
 465 perfect data according to the RainGaugeQC system, is observed in July (summer) and equals 76.1% and 57.6%
 466 for professional and non-professional data respectively, while the percentage of data with poor qualities is also
 467 lowest in this month for both types of the data: 1.4% and 7.2%, respectively. Considering the distribution of QI
 468 values in the different ranges, the data from January proved to be the least reliable, when the percentage of data

469 with low QI values, i.e. in the range between 0.0 and 0.75, is the highest, reaching 4.9% for professional and 24.2%
 470 non-professional data. The low percentage of $QI = 1.0$ in January for both data types is due to the methodology
 471 used to determine these values in the SCC algorithm (Section 3.5). It uses the spatial variability function (SVF),
 472 which quantifies the spatial variability of precipitation at each time step. The high variability of precipitation is
 473 associated with convective precipitation and the introduction of the SVF function is intended to prevent such
 474 precipitation from being treated too rigorously and decreasing QI of good measurements. However, convective
 475 precipitation is very rare in winter in Poland, hence the frequent reduction of QI for weak outliers.

476 4.4 Impact of non-professional rain data on the reliability of precipitation estimates

477 The following data sets were applied to test the influence of non-professional rain data on the reliability of
 478 precipitation estimation: (i) professional only and (ii) professional and non-professional together after quality
 479 control with the modified version of RainGaugeQC. From both rain gauge data sets, 10-min multi-source estimates
 480 of precipitation accumulations were generated with the RainGRS system and then aggregated to the daily
 481 accumulations. Table 3 shows the reliability metrics of the daily accumulations calculated for April, July, October
 482 2023 and January 2024, using the manual rain gauge data as a reference. Statistics were determined at the locations
 483 of the manual rain gauges.

484
 485 **Table 3. Reliability metrics of estimates of daily RainGRS precipitation accumulations generated using rain**
 486 **gauge data: professional and professional with attached data from non-professional rain gauges after**
 487 **quality control with the modified version of RainGaugeQC. Measurements from manual rain gauges are**
 488 **used as a reference, data from April, July, October 2023 and January 2024.**

| Rain gauge networks | CC (-) | RMSE (mm) | RRSE (-) | BIAS (mm) |
|---|-----------|--------------|-------------|--------------|
| <i>April 2023</i> | | | | |
| Professional (IMGW and CHMU) | 0.832 | 2.74 | 0.64 | -1.36 |
| Professional (IMGW and CHMU) and non-professional (State Forests) | 0.872 | 2.40 | 0.55 | -1.11 |
| <i>July 2023</i> | | | | |
| Professional (IMGW and CHMU) | 0.835 | 3.99 | 0.57 | -1.03 |
| Professional (IMGW and CHMU) and non-professional (State Forests) | 0.847 | 3.71 | 0.55 | -0.93 |
| <i>October 2023</i> | | | | |
| Professional (IMGW and CHMU) | 0.920 | 2.35 | 0.43 | -0.91 |
| Professional (IMGW and CHMU) and non-professional (State Forests) | 0.922 | 2.28 | 0.41 | -0.79 |
| <i>January 2024</i> | | | | |
| Professional (IMGW and CHMU) | 0.844 | 2.55 | 0.65 | -1.42 |
| Professional (IMGW and CHMU) and non-professional (State Forests) | 0.846 | 2.52 | 0.64 | -1.40 |

489

490 It can be seen from Table 3 that after the incorporation of non-professional data provided by the General
491 Directorate of the State Forests into RainGRS, all reliability metrics improved. In the four months analysed on
492 average, the correlation coefficient increased only marginally. Greater improvement after the inclusion of non-
493 professional data can be seen in all metrics related to error magnitude: RMSE, RRSE and BIAS, which on average
494 decreased by 0.16 mm, 0.03, and 0.12 mm, respectively.

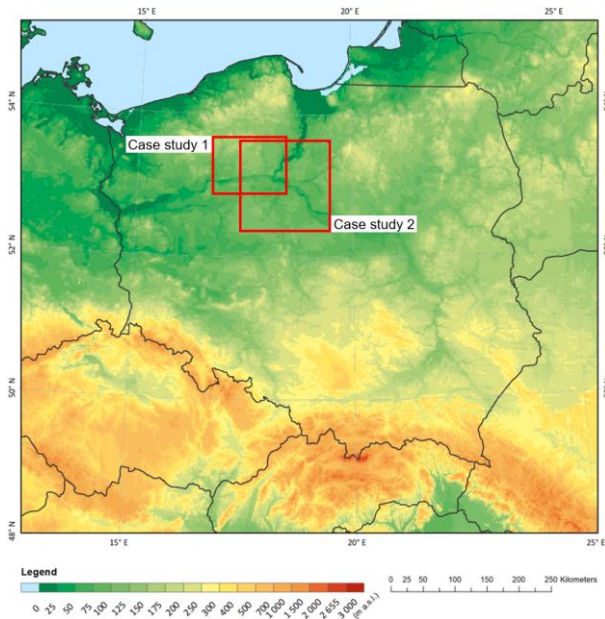
495 Analysing the four metrics used, the most positive impact of incorporating non-professional data was found in
496 April 2023, an intermediate month, when all characteristics improved: CC increased by 0.04, while metrics related
497 to error magnitude improved: RMSE by 0.34 mm, RRSE by 0.09 and BIAS by 0.35 mm. This observation is
498 consistent with the results shown in Fig. 3, where in April the non-professional data were even more reliable than
499 the professional data in terms of CC and RRSE metrics. The smallest impact of non-professional data was observed
500 in January, when the improvement was negligible.

501 It should be pointed out that the number of non-professional rain gauges available for this study was not large:
502 the ratio between the number of rain gauges in the non-professional and professional networks was about 1:4.
503 Therefore, it can be expected that if there were more of these non-professional rain gauges, then the benefit from
504 them in terms of improvement in the reliability of the precipitation estimates would be even more pronounced.
505 This impact is not only due to the measurement information provided by these rain gauges, but also largely due to
506 the fact that additional rain gauges make quality control of all rain gauges much more effective.

507 **4.5 Impact of non-professional rain gauges on estimated multi-source precipitation field – varying impact** 508 **in different locations**

509 This section presents two case studies illustrating the influence of non-professional precipitation data on the
510 reliability of precipitation estimates generated by the RainGRS system. The location of the study areas is shown
511 on a map of Poland (Fig. 5). Locations in central Poland were chosen because the network of professional rain
512 gauges is sparsest there (see Fig. 1), so the influence of non-professional data on the final estimate of the
513 precipitation field can be expected to be more evident. Two different RainGRS precipitation field estimates were
514 generated using rain gauge data: (i) from professional rain gauges only, (ii) from both professional and non-
515 professional rain gauges. The impact of incorporating non-professional rain gauge data on multi-source field
516 estimates was assessed using manual rain gauge measurements as reference data. The analyses were conducted on
517 daily accumulations because only this kind of data are available from manual rain gauges.

518



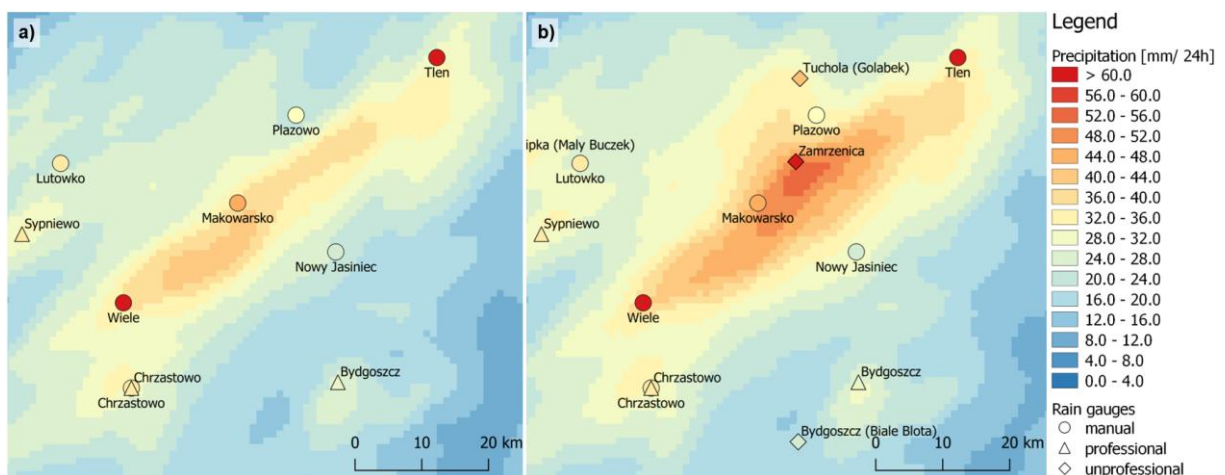
519
520 **Figure 5. Location of case studies on a map of Poland.**

521

522 **4.5.1 Case study 1: isolated convective precipitation (29-30 July 2023)**

523 On 29 and 30 July 2023 Poland was under the influence of a trough of low pressure and atmospheric front systems
524 moving from west to east. There were some showers and thunderstorms with precipitation locally reaching more
525 than 60 mm per day, which triggered flash flooding in major cities in the north of the country. Fig. 6 presents the
526 daily precipitation accumulations for this day, which shows the effect of including non-professional rain gauge
527 data to the input data to the RainGRS model generating multi-source precipitation field estimates.

528



529
530 **Figure 6: Precipitation maps of multi-source RainGRS estimates from: a) professional, b) professional and non-**
531 **professional data. The symbols are filled with colours that correspond to the precipitation values measured by each rain**
532 **gauge. A fragment of Poland, daily accumulations from 29.07.2023, 06 UTC to 30.07.2023, 06 UTC.**

533

534 In the fields of estimated precipitation accumulations in the vicinity of the thunderstorm cell in Fig. 6, it can
535 be seen that after incorporation of the non-professional data, the accumulations became noticeably higher, as the

536 data from the non-professional rain gauges are generally higher than those from the professional ones – a general
537 increase in values can be seen in Fig. 6b compared to Fig. 6a. Using the measurements from the manual rain gauges
538 as reference data, it can be concluded that the obtained increase in the estimated RainGRS precipitation field is
539 closer to the reference precipitation (this is confirmed by the results in Table 3). Regarding the thunderstorm cell
540 moving through the study area, it was compact, small in size (its diameter was about 10 km) and no professional
541 rain gauge was in its path. It was detected by weather radars, so it is visible on the multi-source estimate, but the
542 precipitation values are underestimated compared to the reference precipitation recorded by the manual rain gauges
543 located in the path of this cell.

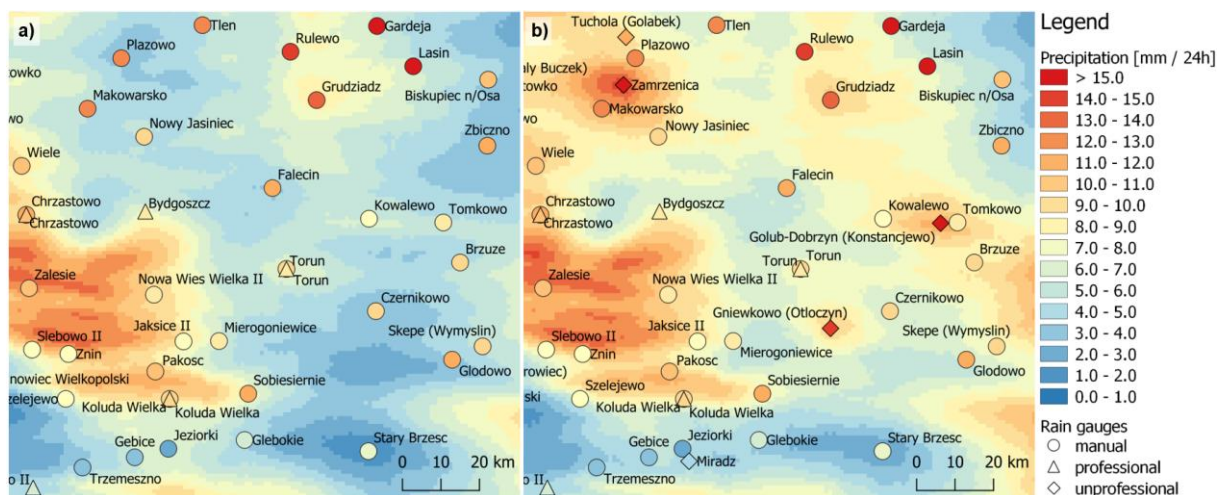
544 When including the non-professional data, a rain gauge in Zamrzenica on the route of this storm cell measured
545 a daily rainfall of 62.3 mm, resulting in a significant increase in the RainGRS precipitation estimate in this area:
546 from 31.6 to 50.6 mm at the Zamrzenica location. However, due to the small number of rain gauges in the area,
547 the high precipitation spread over a much larger region than the close vicinity of the cell. This is evidenced by the
548 lower precipitation measured by the manual rain gauge at Nowy Jasiniec (23.3 mm), while the precipitation
549 estimate increased here from 24.2 to 31.0 mm.

550 Closest to the path of the cell was the Makowarsko manual rain gauge, which measured 46.8 mm. The multi-
551 source estimate after including the non-professional rain gauge increased from 37.8 to 47.1 mm, which is in very
552 good agreement with the reference value. The precipitation estimate at the Płazowo manual rain gauge location
553 also increased: from 22.4 to 33.5 mm, while this rain gauge measured 29.2 mm. The increase in estimates was
554 therefore too high, but nevertheless, after data from non-professional rain gauges were added to the estimate, it
555 was closer to the measurement from the reference rain gauge. The highest value of 68.5 was measured by the Tleń
556 manual rain gauge, but the incorporation of the non-professional data only slightly improved the highly
557 underestimated estimate from 31.5 to 33.7 mm.

558 **4.5.2 Case study 2: winter stratiform precipitation (3-4 January 2024)**

559 At the beginning of January 2024, Poland was in the range of low-pressure systems moving from west to east and
560 associated atmospheric fronts. Rainfall and sleet were observed, with snowfall in the north-east of the country and
561 in the mountains in the south. In the north and centre, there was also freezing rain causing glaze. The example
562 shown in Fig. 7 relates to a lowland area in central Poland, like in the first case study, but here there was stratiform
563 precipitation, which was significantly lower but at a greater extent, as is typical for winter.

564



565
 566 **Figure 7: Precipitation maps of multi-source RainGRS estimates from: a) professional, b) professional and non-**
 567 **professional data. The symbols are filled with colours that correspond to the precipitation values measured by each rain**
 568 **gauge. A fragment of Poland, 24-h accumulations from 3.01.2024, 06 UTC to 4.01.2024, 06 UTC.**

569
 570 The RainGRS precipitation field estimation generated values that were underestimated compared to the manual
 571 rain gauge measurements: the estimated values were lower by 3.2 mm on average, while their daily accumulation
 572 averaged 9.5 mm at the locations of these rain gauges. This is mainly due to the underestimation of weather radar
 573 and, to a lesser extent, telemetric measurements.

574 The inclusion of data from non-professional rain gauges, despite their small number, increased the RainGRS
 575 estimate at manual rain gauge locations by an average of 1.3 mm. For example, it can be seen that that Zamrzenica
 576 non-professional rain gauge had a positive effect on the estimated daily precipitation accumulation (RainGRS) at
 577 the manual rain gauge located in Płazowo, where 12.1 mm was measured, and the estimates with and without the
 578 incorporation of non-professional data were 9.5 and 3.3 mm, respectively.

579 The impact of the Miradz non-professional rain gauge was slightly different. It measured a value of 3.1 mm
 580 and caused the estimates at the location of the two closest manual rain gauges to decrease at Jeziorki from 6.7 to
 581 4.7 mm, and at Gębice from 6.0 to 4.9 mm, approaching the values from the manual rain gauges of 1.7 and 3.0
 582 mm respectively. On the other hand, the influence of Miradz appeared to negatively affect the estimates at the
 583 manual rain gauge locations of Koluda Wielka and Szelejewo, where values that had been underestimated
 584 compared to the reference rainfall were lowered even further.

585 The analysis of the two case studies indicates that data from non-professional rain gauges, despite their
 586 generally higher uncertainty, can positively contribute to estimating the precipitation field in many cases.

587 5 Conclusions

588 Data from non-professional rain gauge networks, as additional source of precipitation data, increase the density of
 589 available rain gauge networks. In consequence they can improve precipitation field estimates at high spatial
 590 resolution and can be very helpful to NHMSs for various meteorological and hydrological applications. However,
 591 advanced data quality control systems are required to make these data useful for operational applications. At the

592 same time, it should be possible to objectively quantify the uncertainty associated with each individual
593 measurement.

594 The RainGaugeQC system, applied to quality control of rain gauge data, was redesigned in order to adapt it to
595 different rain gauge networks supervised to various degrees. In a modified version of the TCC algorithm, more
596 sophisticated data control was developed applying weather radar data, taking into account various aspects of data
597 quality, such as consistency analysis of data time series. The new BC algorithm was introduced to detect bias of
598 rain gauge measurements comparing rain gauge and radar long-term accumulations. In the SCC algorithm,
599 significant modifications have been made to quantify the quality index reduction for outliers on the basis of the
600 spatial variability of the precipitation field derived from the radar data. The performance of the modified system
601 was verified based on independent measurement data from manual rain gauges, which are considered one of the
602 most accurate measurement instruments. The influence of incorporating non-professional precipitation data on
603 reliability of multi-source precipitation estimates generated by the RainGRS system was also analysed.

604 The main conclusions derived from the analyses carried out in this study can be summarised as follows:

- 605 1. The incorporation of data from non-professional stations into professional rain gauge data, even if they
606 are of poorer quality (Fig. 4), nevertheless improves the reliability of the estimated multi-source
607 precipitation field (Table 3), but on the condition that advanced quality control is carried out.
- 608 2. Despite the quality control performed, the influence of individual rain gauges on the precipitation field
609 estimates may sometimes not be positive, as can be seen from the examples shown in Section 4.5.
610 Furthermore, the same rain gauge may have a different influence, positive or negative, on an estimated
611 precipitation field in various places.
- 612 3. An important benefit of including data from non-professional networks is the improvement in
613 performance of individual QC algorithms. This is especially true for the spatial consistency check (SCC),
614 in which the density of a rain gauge network is crucial.

615 The development of the quality control system for telemetric rain gauge measurements will be continued.
616 Plans include incorporating precipitation data from other non-professional networks to supplement the IMGW rain
617 gauge network. This will increase the proportion of data with potentially lower reliability, which may require even
618 more sophisticated algorithms for the quality control. Moreover, IMGW is in the process of establishing a network
619 of personal rain gauges. Once this network is operational, it will be possible to test the quality control algorithms
620 proposed in this paper using data from these rain gauges.

621 **Acknowledgement**

622 The work described in this paper was carried out primarily within the COSMO consortium (Consortium for Small-
623 scale Modelling) as Priority Task EPOCS “Evaluate Personal Weather Station and Opportunistic Sensor Data
624 Crowdsourcing” during the period 2023-2024.

625
626 *Code availability.* The data processing codes are protected through the economic property rights to the software
627 and are not available for distribution. The codes used for processing follow the methodologies and equations
628 described herein.

629
630 *Data availability.*

631 Out of the data used in this article, the following are publicly available:
632 IMGW rain gauge data in the form of 10-minute accumulations: <https://danepubliczne.imgw.pl/pl/datastore>, tabs:
633 „Dane archiwalne” / „Dane meteorologiczne” / „year” / „Meteo_year-month.zip” / „B00608S_year_month.csv”
634 (B00608S is the code for the 10-min rainfall parameter).
635 Radar data as 1-h files of precipitation accumulation (PAC) maps: <https://danepubliczne.imgw.pl/pl/datastore>,
636 tabs: „Dane archiwalne” / „Mapa zbiorcza sumy opadów za godzinę.” / „year” / „month” /
637 COMPO_PAC.comp.pac_year-month-day.tar.
638 Other data used in this article is available upon request, provided it is not restricted by its producer.

639
640 *Author contributions.* KO, JS, and AJ designed algorithms of the RainGaugeQC system. KO developed the
641 software code and performed the simulations. JS, KO, AJ, and AK prepared the paper. JS made figures. AK carried
642 out statistical calculations.

643
644 *Competing interests.* The contact author has declared that none of the authors has any competing interests.

645 **References**

- 646 Alerskans, E., Lussana, C., Nipen, T. N., and Seierstad, I. A.: Optimizing Spatial Quality Control for a Dense
647 Network of Meteorological Stations, *Journal of Atmospheric and Oceanic Technology*, 39, 973–984,
648 [doi:10.1175/JTECH-D-21-0184.1](https://doi.org/10.1175/JTECH-D-21-0184.1), 2022.
- 649 Bárdossy, A., Seidel, J., and El Hachem, A.: The use of personal weather station observation for improving
650 precipitation estimation and interpolation, *Hydrology and Earth System Sciences*, 25, 583–601,
651 [doi:10.5194/hess-25-583-2021](https://doi.org/10.5194/hess-25-583-2021), 2021.
- 652 Båserud, L., Lussana, C., Nipen, T. N., Seierstad, I. A., Oram, L., and Aspelien, T.: TITAN automatic spatial
653 quality control of meteorological in-situ observations, *Advances in Science and Research*, 17, 153–163,
654 [doi:10.5194/asr-17-153-2020](https://doi.org/10.5194/asr-17-153-2020), 2020.
- 655 Bell, S., Cornford, D., and Bastin, L.: How good are citizen weather stations? Addressing a biased opinion,
656 *Weather*, 70, 75–84, [doi:10.1002/wea.2316](https://doi.org/10.1002/wea.2316), 2015.
- 657 Berndt, C., and Haberlandt, U.: Spatial interpolation of climate variables in Northern Germany –Influence of
658 temporal resolution and network density, *Journal of Hydrology: Regional Studies*, 15, 184–202,
659 [doi:10.1016/j.ejrh.2018.02.002](https://doi.org/10.1016/j.ejrh.2018.02.002), 2018.
- 660 Chwala, C., and Kunstmann, H.: Commercial microwave link networks for rainfall observation: assessment of the
661 current status and future challenges. *Wiley Interdisciplinary Reviews: Water*, 6, e1337. [doi:10.1002/wat2.1337](https://doi.org/10.1002/wat2.1337),
662 2019.
- 663 Colli, M., Lanza, L.G., La Barbera, P., and Chan, P.W.: Measurement accuracy of weighing and tipping-bucket
664 rainfall intensity gauges under dynamic laboratory testing, *Atmospheric Research*, 144, 186–194,
665 [doi:10.1016/j.atmosres.2013.08.007](https://doi.org/10.1016/j.atmosres.2013.08.007), 2014.
- 666 de Vos, L., Leijnse, H., Overeem, A., and Uijlenhoet, R.: The potential of urban rainfall monitoring with
667 crowdsourced automatic weather stations in Amsterdam. *Hydrology and Earth System Sciences*, 21, 765–777,
668 [doi:10.5194/hess-21-765-2017](https://doi.org/10.5194/hess-21-765-2017), 2017.

669 de Vos, L. W., Leijnse, H., Overeem, A., and Uijlenhoet, R.: Quality control for crowdsourced personal weather
670 stations to enable operational rainfall monitoring. *Geophysical Research Letters*, 46, 8820–8829,
671 [doi:10.1029/2019GL083731](https://doi.org/10.1029/2019GL083731), 2019.

672 Drożdżioł, R., and Absalon, D.: Evaluation of selected amateur rain gauges with Hellmann rain gauge
673 measurements. *Climate*, 11, 107, [doi:10.3390/cli11050107](https://doi.org/10.3390/cli11050107), 2023.

674 Garcia-Marti, I., Overeem, A., Noteboom, J. W., de Vos, L., de Haij, M., and Whan, K.: From proof-of-concept
675 to proof-of-value: Approaching third-party data to operational workflows of national meteorological services.
676 *International Journal of Climatology*, 43, 275–292, [doi:10.1002/joc.7757](https://doi.org/10.1002/joc.7757), 2023.

677 Graf, M., El Hachem, A., Eisele, M., Seidel, J., Chwala, C., Kunstmann, H., and Bárdossy, A.: Rainfall estimates
678 from opportunistic sensors in Germany across spatio-temporal scales. *Journal of Hydrology: Regional Studies*,
679 37, 100883, [doi:10.1016/j.ejrh.2021.100883](https://doi.org/10.1016/j.ejrh.2021.100883), 2021.

680 Hahn, C., Garcia-Marti, I., Sugier, J., Emsley, F., Beaulant, A.-L., Oram, L., Strandberg, E., Lindgren, E., Sunter,
681 M., and Ziska, F.: Observations from Personal Weather Stations – EUMETNET Interests and Experience,
682 *Climate*, 10, 192, [doi:10.3390/cli10120192](https://doi.org/10.3390/cli10120192), 2022.

683 Haselow, L., Meissner, R., Rupp, H., and Miegel, K.: Evaluation of precipitation measurements methods under
684 field conditions during a summer season: A comparison of the standard rain gauge with a weighable lysimeter
685 and a piezoelectric precipitation sensor, *Journal of Hydrology*, 575, 537–543,
686 [doi:10.1016/j.jhydrol.2019.05.065](https://doi.org/10.1016/j.jhydrol.2019.05.065), 2019.

687 Hoffmann, M., Schwartengraber, R., Wessolek, W., and Peters, A.: Comparison of simple rain gauge
688 measurements with precision lysimeter data, *Atmospheric Research*, 174-175, 120-123,
689 [doi:10.1016/j.atmosres.2016.01.016](https://doi.org/10.1016/j.atmosres.2016.01.016), 2016.

690 Hohmann, C., Kirchengast, G., O, S., Rieger, W., and Foelsche, U.: Small catchment runoff sensitivity to station
691 density and spatial interpolation: hydrological modeling of heavy rainfall using a dense rain gauge network,
692 *Water*, 13, 1381, [doi:10.3390/w13101381](https://doi.org/10.3390/w13101381), 2021.

693 Horita, F. E. A., Vilela, R. B., Martins, R. G., Bressiani, D. A., Palma, G., and Porto de Albuquerque, J.:
694 Determining flooded areas using crowd sensing data and weather radar precipitation: a case study in Brazil. In:
695 ISCRAM 2018, Rochester, NY, USA, 20-23 May 2018. Published in: Proceedings of the 15th ISCRAM
696 Conference – Rochester, NY, USA May 2018, 1040-1050, 2018.

697 Jurczyk, A., Szturc, J., and Ośródk, K.: Quality-based compositing of weather radar QPE estimates,
698 *Meteorological Applications*, 27, e1812, [doi:10.1002/met.1812](https://doi.org/10.1002/met.1812), 2020a.

699 Jurczyk, A., Szturc, J., Otop, I., Ośródk, K., and Struzik, P.: Quality-based combination of multi-source
700 precipitation data. *Remote Sensing*, 12, 1709, [doi:10.3390/rs12111709](https://doi.org/10.3390/rs12111709), 2020b.

701 Jurczyk, A., Ośródk, K., Szturc, J., Pasierb, M., and Kurcz, A.: Long-term multi-source precipitation estimation
702 with high resolution (RainGRS Clim), *Atmospheric Measurement Techniques*, 16, 4067–4079,
703 [doi:10.5194/amt-16-4067-2023](https://doi.org/10.5194/amt-16-4067-2023), 2023.

704 Krennert Th., Pistotnik G., Kaltenberger R., and Csekits C.: Crowdsourcing of weather observations at national
705 meteorological and hydrological services in Europe, *Advances in Science and Research*, 15, 71–76,
706 [doi:10.5194/asr-15-71-2018](https://doi.org/10.5194/asr-15-71-2018), 2018.

707 Lanza, L. G. and Vuerich, E.: The WMO Field Intercomparison of Rain Intensity Gauges, *Atmospheric Research*,
708 94, 534-543, [doi:10.1016/j.atmosres.2009.06.012](https://doi.org/10.1016/j.atmosres.2009.06.012), 2009.

709 Loritz, R., Hrachowitz, M., Neuper, M., and Zehe, E.: The role and value of distributed precipitation data in
710 hydrological models, *Hydrology and Earth System Sciences*, 25, 147–167, [doi:10.5194/hess-25-147-2021](https://doi.org/10.5194/hess-25-147-2021),
711 2021.

712 McKee, J. L. and Binns, A. D.: A review of gauge–radar merging methods for quantitative precipitation estimation
713 in hydrology, *Canadian Water Resources Journal / Revue Canadienne des Ressources Hydriques*, 41, 186-203,
714 [doi:10.1080/07011784.2015.1064786](https://doi.org/10.1080/07011784.2015.1064786), 2016.

715 Muller, C. L., Chapman, L., Johnston, S., Kidd, C., Illingworth, S., Foody G., Overeem, and A., Lei, R. R.:
716 Crowdsourcing for climate and atmospheric sciences: current status and future potential. *International Journal*
717 *of Climatology*, 35, 3185-3203, [doi:10.1002/joc.4210](https://doi.org/10.1002/joc.4210), 2015.

718 Nipen, T. N., Seierstad, I.A., Lussana, C., Kristiansen, J., and Hov, Ø.: Adopting citizen observations in operational
719 weather prediction. *Bulletin of American Meteorological Society*, 101, E43-E47, [doi:10.1175/BAMS-D-18-](https://doi.org/10.1175/BAMS-D-18-0237.1)
720 [0237.1](https://doi.org/10.1175/BAMS-D-18-0237.1), 2020.

721 Ośródką K., Szturc J., and Jurczyk A.: Chain of data quality algorithms for 3-D single-polarization radar
722 reflectivity (RADVOL-QC system). *Meteorological Applications*, 21, 256–270, [doi:10.1002/met.1323](https://doi.org/10.1002/met.1323), 2014.

723 Ośródką, K. and Szturc, J.: Improvement in algorithms for quality control of weather radar data (RADVOL-QC
724 system), *Atmospheric Measurement Techniques*, 15, 261-277, [doi:10.5194/amt-15-261-2022](https://doi.org/10.5194/amt-15-261-2022), 2022.

725 Ośródką, K., Otop, I., and Szturc, J.: Automatic quality control of telemetric rain gauge data providing quantitative
726 quality information (RainGaugeQC), *Atmospheric Measurement Techniques*, 15, 5581–5597,
727 [doi:10.5194/amt-2022-83](https://doi.org/10.5194/amt-2022-83), 2022.

728 Overeem, A., Leijnse, H., van der Schrier, G., van den Besselaar, E., Garcia-Marti, I., and de Vos, L.: Merging
729 with crowdsourced rain gauge data improves pan-European radar precipitation estimates, *Hydrology and Earth*
730 *System Sciences*, 28, 649–668, [doi:0.5194/hess-28-649-2024](https://doi.org/10.5194/hess-28-649-2024), 2024.

731 Pasierb, M., Baldysz, Z., Szturc, J., Nykiel, G., Jurczyk, A., Ośródką, K., Figurski, M., Wojtczak, M., and
732 Wojtkowski, C.: Application of commercial microwave links (CMLs) attenuation for quantitative estimation
733 of precipitation, *Meteorological Applications*, 31, e2218. [doi:10.1002/met.2218](https://doi.org/10.1002/met.2218), 2024.

734 Polz, J., Chwała, C., Graf, M., and Kunstmann, H.: Rain event detection in commercial microwave link attenuation
735 data using convolutional neural networks, *Atmospheric Measurement Techniques*, 13, 3835–3853.
736 [doi:10.5194/amt-13-3835-2020](https://doi.org/10.5194/amt-13-3835-2020), 2020.

737 Schnepfer, T., Groh, J., Gerke, H. H., Reichert, B., and Pütz, T.: Evaluation of precipitation measurement methods
738 using data from a precision lysimeter network, *Hydrology and Earth System Sciences*, 27, 3265–3292,
739 [doi:10.5194/hess-27-3265-2023](https://doi.org/10.5194/hess-27-3265-2023), 2023.

740 Segovia-Cardozo, D.A., Rodríguez-Sinobas, L., Díez-Herrero, A., Zubezu, S., and Canales-Ide, F.: Understanding
741 the Mechanical Biases of Tipping-Bucket Rain Gauges: A Semi-Analytical Calibration Approach, *Water*, 13,
742 2285, [doi:10.3390/w13162285](https://doi.org/10.3390/w13162285), 2021.

743 Sha, Y., Gagne II, D. J., West, G., and Stull, R.: Deep-Learning-Based Precipitation Observation Quality Control,
744 *Journal of Atmospheric and Oceanic Technology*, 38, 1075–1091, [doi:10.1175/JTECH-D-20-0081.1](https://doi.org/10.1175/JTECH-D-20-0081.1), 2021.

745 Sinclair, S. and Pegram, G.: Combining radar and rain gauge rainfall estimates using conditional merging,
746 *Atmospheric Science Letters*, 6, 19–22, [doi:10.1002/asl.85](https://doi.org/10.1002/asl.85), 2005.

747 Sokol, Z., Szturc, J., Orellana-Alvear, J., Popová, J., Jurczyk, A., and Céleri, R.: The role of weather radar in
748 rainfall estimation and its application in meteorological and hydrological modelling – A review, *Remote*
749 *Sensing*, 13, 351, [doi:10.3390/rs13030351](https://doi.org/10.3390/rs13030351), 2021.

750 Szturc, J., Jurczyk, A., Ośródk, K., Wyszogrodzki, A., and Giszterowicz, M.: Precipitation estimation and
751 nowcasting at IMGW (SEiNO system), *Meteorology Hydrology and Water Management*, 6, 3–12,
752 [doi:10.26491/mhwm/76120](https://doi.org/10.26491/mhwm/76120), 2018.

753 Szturc, J., Ośródk, K., Jurczyk, A., Otop, I., Linkowska, J., Bochenek, B., and Pasierb, M.: Quality control and
754 verification of precipitation observations, estimates, and forecasts, in: *Precipitation Science. Measurement,*
755 *Remote Sensing, Microphysics and Modeling*, edited by S. Michaelides, Elsevier 2022, 91-133,
756 [doi:10.1016/B978-0-12-822973-6.00002-0](https://doi.org/10.1016/B978-0-12-822973-6.00002-0), 2022.

757 Urban, G., Strug, K.: Evaluation of precipitation measurements obtained from different types of rain gauges,
758 *Meteorologische Zeitschrift*, 30, 445-463. [doi:10.1127/metz/2021/1084](https://doi.org/10.1127/metz/2021/1084), 2021.

759 Urban, G., Kowalewski, M.K., Sawicki, J., and Borowiecki, K.: Assessment of the quality of measurements from
760 selected amateur rain gauges, *Meteorologische Zeitschrift*, 33, 159–174, [doi:10.1127/metz/2024/1199](https://doi.org/10.1127/metz/2024/1199), 2024.

761 Van Andel, N., 2021. *Quality control development for near real-time rain gauge networks for operational rainfall*
762 *monitoring*, Master Thesis, Faculty of Physics, Utrecht University, Utrecht,
763 <https://studenttheses.uu.nl/handle/20.500.12932/40939>.

764 Villalobos-Herrera, R., Blenkinsop, S., Guerreiro, S. B., O'Hara, T., and Fowler, H. J.: Sub-hourly resolution
765 quality control of rain gauge data significantly improves regional sub-daily return level estimates, *Quarterly*
766 *Journal of the Royal Meteorological Society*, 148, 3252–3271, [doi:10.1002/qj.4357](https://doi.org/10.1002/qj.4357), 2022.

767 WMO-No. 488, 2010 (updated in 2017). *Guide on the Global Observing System*, World Meteorological
768 Organization, Geneva, 215 pp., ISBN 978-92-63-10488-5,
769 https://library.wmo.int/index.php?lvl=notice_display&id=12516#.Y1QxleTP2Uk, 2015.

770 WMO-No. 1257, 2024. *Guide to Operational Weather Radar Best Practices*. Volume VI: *Weather Radar Data*
771 *Processing*, World Meteorological Organization, Geneva, 166 pp., [https://community.wmo.int/en/activity-](https://community.wmo.int/en/activity-areas/imop/new-provisional-2024-edition-guide-operational-weather-radar-best-practices)
772 [areas/imop/new-provisional-2024-edition-guide-operational-weather-radar-best-practices](https://community.wmo.int/en/activity-areas/imop/new-provisional-2024-edition-guide-operational-weather-radar-best-practices), 2024 (provisional
773 edition).

774 Wood, S. J., Jones, D. A., and Moore, R. J.: Accuracy of rainfall measurement for scales of hydrological interest,
775 *Hydrology and Earth System Sciences*, 4, 531–543, [doi:10.5194/hess-4-531-2000](https://doi.org/10.5194/hess-4-531-2000), 2000.

776 Yan, Q., Zhang, B., Jiang, Y., Liu, Y., Yang, B., and Wang, H.: Quality control of hourly rain gauge data based
777 on radar and satellite multi-source data. *Journal of Hydroinformatics*, 26, 1042–1058,
778 [doi:10.2166/hydro.2024.272](https://doi.org/10.2166/hydro.2024.272), 2024.

779 Yousefi, K. P., Yilmaz, M. T., Öztürk, K., Yucel, I., and Yilmaz, K. Y.: Time-independent bias correction methods
780 compared with gauge adjustment methods in improving radar-based precipitation estimates, *Hydrological*
781 *Sciences Journal*, 68, 1963-1983, [doi:10.1080/02626667.2023.2248108](https://doi.org/10.1080/02626667.2023.2248108), 2023.

782 Zhang, Y., Ren, Y., Ren, G., and Wang G.: Bias Correction of Gauge Data and its Effect on Precipitation
783 Climatology over Mainland China, *Journal of Applied Meteorology and Climatology*, 58, 2177–2196,
784 [doi:10.1175/JAMC-D-19-0049.1](https://doi.org/10.1175/JAMC-D-19-0049.1), 2019.

785 Zheng, F., Tao, R., Maier, H. R., See, L., Savic, D., and Zhang, T., et al.: Crowdsourcing methods for data
786 collection in geophysics: State of the art, issues, and future directions, *Reviews of Geophysics*, 56, 698–740.
787 [doi:10.1029/2018RG000616](https://doi.org/10.1029/2018RG000616), 2018.